Ceramics-Silikáty 66 (4), 540-554 (2022)
www.ceramics-silikaty.cz doi: 10.13168/cs.2022.0050

EFFECTS OF DESERT SAND SUBSTITUTION ON CONCRETE PROPERTIES USING DESERT SAND-DOPED ARTIFICIAL SAND AS THE FINE AGGREGATE

TAICHANG LIAO*, **, XIN HUANG***, JIE YUAN***, SHAOQIANG REN*, HE CAI*, **, #XIN CHEN***

*China Railway 20th Bureau Group Co., Ltd., Xi'an 710016, P. R. China
**China Railway Construction Technology Testing Co., Ltd., Xi'an 710016, P. R. China
***School of Transportation Science and Engineering, Harbin Institute of Technology, Harbin 150090, P. R. China

#E-mail: xin.chen@alu.hit.edu.cn

Submitted September 10, 2022; accepted November 6, 2022

Keywords: Concrete, Desert sand, Artificial sand, Strength, Durability, Shrinkage, Microstructure

As governments are increasingly attaching more importance to environmental protection, many policies and regulations are being promulgated to restrict or prohibit river sand extraction. Thus, there is a growing tendency for concrete production to use desert sand-doped artificial sand as the fine aggregate. This paper investigated the microstructure, mechanical properties, durability, and volume stability of concrete with desert sand and artificial sand. In the study, the strength grades of concrete ranged from C30 to C100, while the substitution ratios of the desert sand for the artificial sand ranged from 0 % to 100 %. The results showed that a high substitution ratio of desert sand increased the concrete porosity and extended the interface zone width. The concrete strength generally decreased as the desert sand substitution ratio increased, however, for the C50 and C60 strength grades, concrete with 20 % desert sand had minor positive effects. Basically, as the desert sand substitution ratio increased, the Cl- penetration resistance and frost resistance tended to be weaker, although there were a few exceptions. High substitution ratios of desert sand were also not good for the sulfate attack resistance of concrete. In most cases, concrete with 20 % desert sand shrank more slowly than concrete without desert sand. These conclusions provide the experimental support for the promotion of desert sand applications in the concrete industry.

INTRODUCTION

In developing countries, there is a huge amount of infrastructure engineering projects either in process or in the planning stage, thus building materials including sand, as a concrete fine aggregate, are in great demand [1]. However, the adverse impact of river sand extraction on the ecological environment has been recognised [2]. In order to protect the ecological environment of natural rivers, governments have promulgated a series of policies and regulations to restrict or even prohibit sand extraction in natural rivers [3]. Consequently, construction enterprises are scrambling to find alternatives to river sand. Sea sand had always been an alternative, but later people found that sea sand from different sources had huge differences in its physical and mechanical properties [4]. Desert sand is another alternative, which is abundant in desert regions [5]. Zhang verified that desert sand can be used as a fine aggregate in common mortar and concrete [6]. However, as the size of desert sand is very small, it was better to blend with other sand, otherwise, it was hard to produce high-performance concrete [7]. Wang successfully used desert sand-doped quartz sand as the fine aggregates to produce ultra-high-performance concrete (UHPC) with high tensile strength having very good resistance to freeze-thaw cycling [8]. Similarly, Jiang also successfully used desert sand-doped river sand to produce UHPC with high compressive strength [9].

Recently, researchers and engineers have begun to use desert sand as a substitution for artificial sand to produce concrete, as desert sand has the potential to fill the gap between artificial sand particles, the distribution of which is always discontinuous due to the lack of fine particles [10, 11]. Many strength prediction models have been built based on experimental statistics or various theories, for example, heterogeneous nucleation [12], harmful capillaries [13], and compressible accumulation [14]. Most research about desert sand applications in concrete technology took the desert sand substitution ratio as being univariate, while the sand ratio and other indices of the mix proportion were controlled to be constant. Consequently, the workability and moulding quality of concrete were negatively affected as the substitution ratio increased, making concrete infeasible for engineering applications [15-18]. In this study, the concrete properties using desert sand-doped artificial sand were investigated with the premise that the mix proportions were adjusted to acquire the expected strength grades and fluidities, which are two of the most

important indices in engineering activities. Both the desert sand substitution ratios and the strength grades covered wide ranges, respectively, from C30 to C100 and from 0 % to 100 %. The research outcomes provide the experimental support for the promotion of desert sand applications in the concrete industry.

EXPERIMENTAL

Raw materials

The binders in this study included P-O 42.5 Portland cement, secondary fly ash (FA), and silica fume (SF). FA is widely used in concrete engineering, while SF is also commonly used in high strength concrete production. In this study, the SiO_2 content of the SF in the study was 91.5 %, and the specific area of the SF was 19 300 $m^2 \cdot kg^{-1}$.

The fine aggregates in this study include artificial sand (AS) and desert sand (DS). The AS was made of limestone, while the DS was from the Mu Us Desert, located in northwest China. Magnified photos of the desert sand particles showed that they had smooth surfaces with few open pores, see Figure 1. The particle-size distribution of the DS is shown in Table 1. The diameters of most of the DS particles were in the range of 100 ~ 250 μm. The technical parameters of the AS and DS are shown in Table 1. Both the AS and the DS were confirmed to have no risk of an alkaline-silica reaction, see Appendix A.

The coarse aggregate in this study was continuous grading crushed stone. The particle-size ranges were different for the different strength grade concrete. For the C30 concrete, the particle size ranged from 5 mm to 31.5 mm. For the C50 and higher strength grade concrete, the particle size ranged from 5 mm to 20 mm.

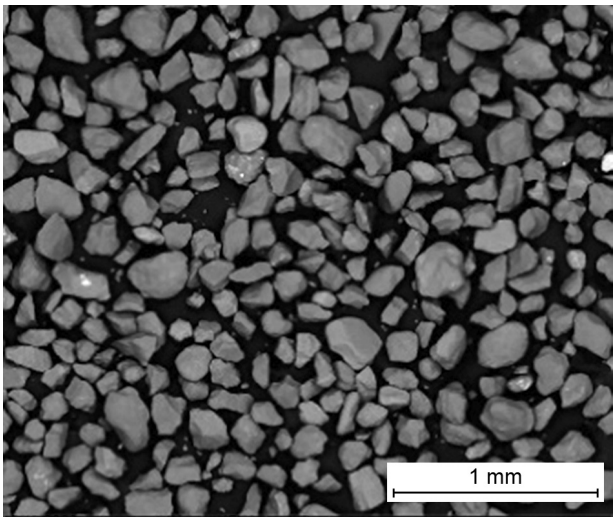

a) General morphology

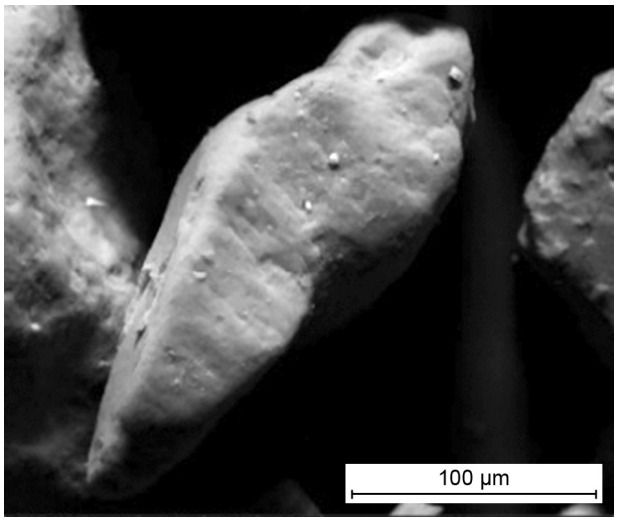

b) Quartz particle

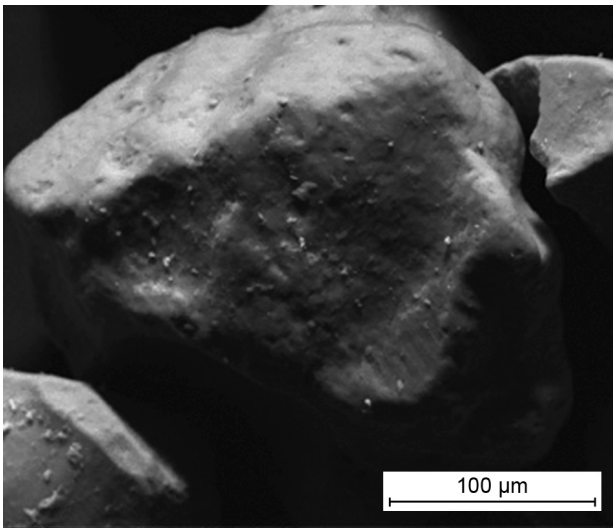

c) Albite particle

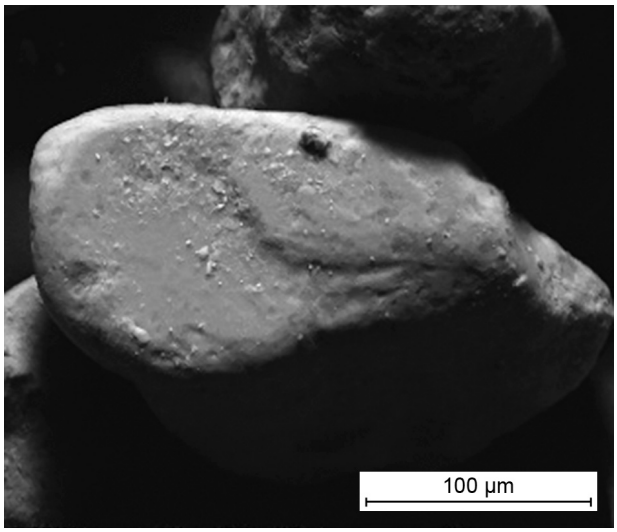

d) Potassium feldspar particle

Figure 1. Magnified photos of the desert sand particles.

Table 1. Technical parameters of the AS and DS.

Sand	Fineness modulus	Stone powder content (%)	Clay content (%)	Water absorption rate at a saturated surface dry state (%)
AS	3.0	6.139	–	1.27
DS	0.71	–	0.574	0.44

A polycarboxylate superplasticiser was applied as the chemical admixture of the concrete in this study.

Mix proportion

The main difference between this study and other studies in the methodology was the principle of the mix proportion design of the concrete with desert sand. It should be pointed out that this research is not a strictly univariate investigation about the desert sand substitution. All the mix proportions of the concrete investigated should meet the requirements of actual engineering practice, at least the requirements of the strength grade and fluidity. Firstly, as the desert sand substitution ratio increased, more cement paste was needed to wrap the fine aggregate, otherwise, the sand ratio should decrease [19]. Secondly, it is known that the concrete workability is adversely affected by the desert sand substitution, however, modern engineering projects have faced the high demand for concrete workability [20]. Thus, the sand ratio should decrease to keep the concrete fluidity if the desert sand substitution ratio increases. Thirdly, as the demand for the strength grade increases, the binder composition and content, binder/cement ratio, and the sand ratios must be regulated [21].

The different strength concrete grades had different binder compositions, binder contents, and binder/cement ratios. The mix proportions of the cement paste for the concrete using desert sand-doped artificial sand as the fine aggregate (DAS concrete) in this study are listed in Table 2, while the binder compositions are shown in Figure 2a.

Besides the cement paste, the residual space in the concrete was occupied by the aggregate, including the fine aggregate (sand) and coarse aggregate (crushed stone). The sand ratios of the concrete with the different strength grades and different desert sand substitution ratios are shown in Figure 2b.

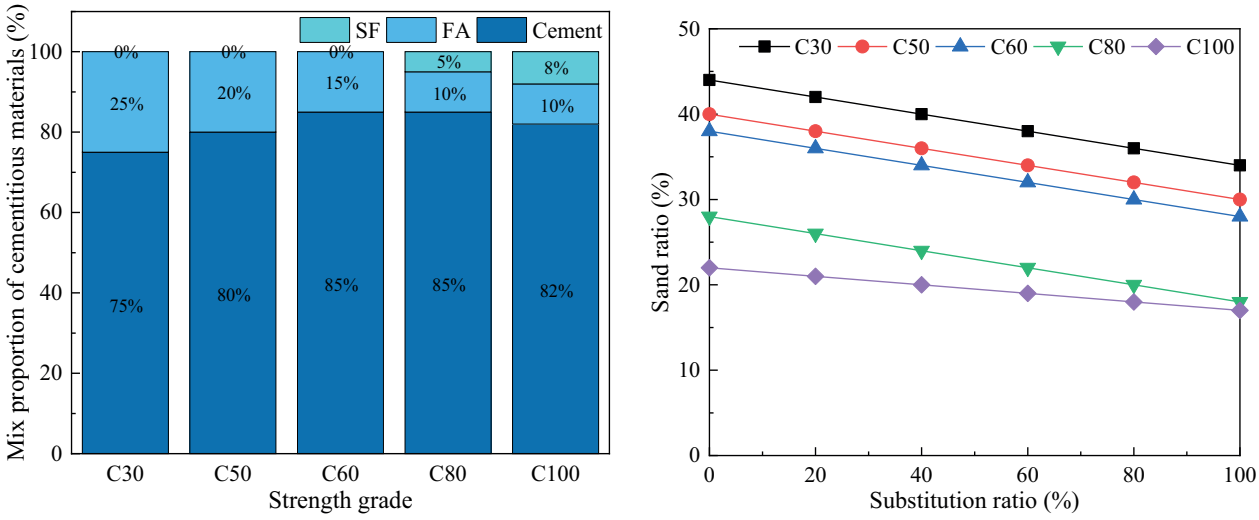

a) binders b) aggregate

Figure 2. Mix compositions of the binders and aggregate of the DAS concrete.

Table 2. Mix proportion of the cement paste for the DAS concrete.

	Binder ($kg \cdot m^{-3}$)	Water ($kg \cdot m^{-3}$)	Superplasticizer ($kg \cdot m^{-3}$)	w/b ratio	Superplasticizer content
C30	377	168	3.77	0.45	1 %
C50	476	146	4.76	0.31	1 %
C60	493	138	4.93	0.28	1 %
C80	580	135	5.80	0.23	1 %
C100	610	132	6.10	0.22	1 %

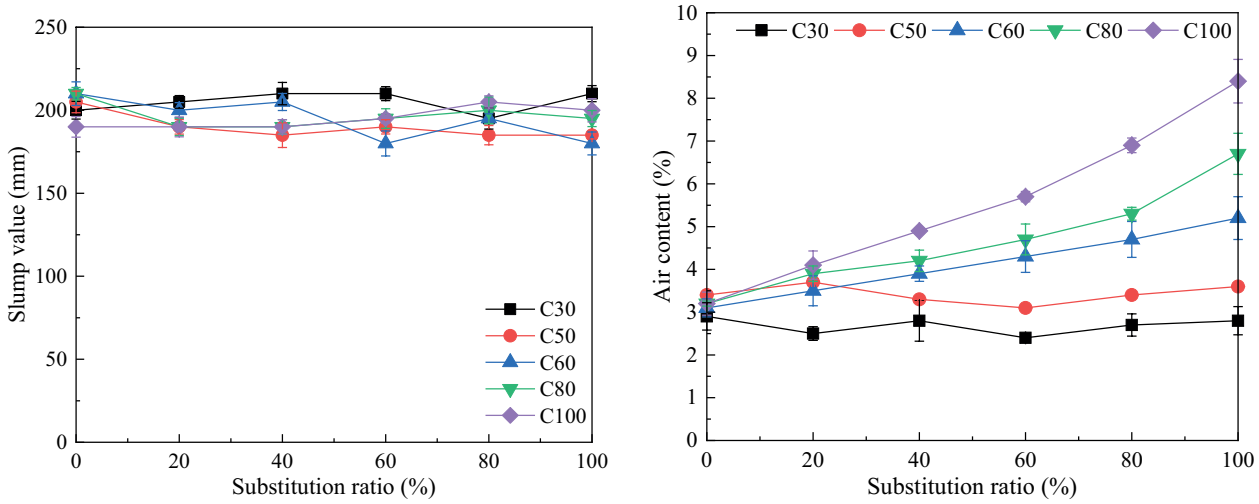

a) fluidity b) air content

Figure 3. Fresh DAS concrete properties.

Fluidity and air content of the freshly designed concrete

The control index for the fluidity in this study was the slump value. The slump values for all the concrete in the study were controlled at a range between 190 mm and 210 mm, see Figure 3a. The slump values proved that the concrete designed had good workability. In addition, the air content of the concrete varied with the mix proportion variation. The air content of designed concrete is shown in Figure 3b. It can be seen that the air content increased as the strength grade increased, while for the high strength concrete (≥ C60), the air content also increased as the desert sand substitution ratio increased.

Test methods

Microstructure tests

The microstructure tests included a pore structure analysis and an interface zone (ITZ) microhardness test.

The pore structure analysis of the concrete used mortar specimens, which had the same mix proportion of the corresponding concrete, except that there was no coarse aggregate. The specimen diameter was controlled at about 5 mm. The analysis was conducted by mercury intrusion porosimetry (MIP) using an AutoPore IV 9500 automatic mercury porosimeter.

ITZ microhardness test was conducted by an HXS-1000AC microhardness tester. Test points were distributed from the coarse aggregate edge to the cement stone matrix at intervals of 10 μm.

Strength test

The compressive strength test of the concrete was conducted in accordance with GB/50081-2019: Standard for test methods of concrete physical and mechanical properties. The specimens were 150 × 150 × 150 mm concrete cubes, while the loading rate was 2.4 $kN \cdot s^{-1}$.

Durability and shrinkage tests

The durability and shrinkage tests were conducted in accordance with GB/T 50082-2009: Standard for test methods of long-term performance and durability of ordinary concrete.

The durability tests in this study included a Cl^- penetration test, a frost resistance test, and a sulfate attack resistance test. (i) The Cl^- penetration test was conducted by the electric flux method instead of the Cl^- diffusion coefficient method. The test lasted for 6 hours under 60 V DC Voltage. (ii) The frost resistance test was conducted by a quick method. Each freeze-thaw cycle lasted for 2 to 4 hours. In a freeze-thaw cycle, the central temperature of the concrete prism was in the range of –18 °C to 5 °C. (iii) The sulfate attack resistance test was coupled with the wet-dry cycles. The concentration of the Na_2SO_4 solution was 5 %.

The shrinkage test was conducted by the contact method. The shrinkage of the concrete prism was measured by a dial gauge and recorded from the age of 1 d to 360 d.

RESULTS AND DISCUSSION

Microstructure of the AS, DAS and DS concrete

MIP of the AS, DAS and DS concrete

The Mercury intrusion porosimetry results of the mortar from AS, DAS* (50 % DS + 50 % AS), and DS concrete are shown in Figure 4 and Figure 5. Figure 4 shows the log differential intrusion curves, while Figure 5 shows the cumulative intrusion curves.

In Figure 4, the log differential intrusion curves of the AS, DAS*, and DS concrete followed similar directions. At the pore diameter range between 100 nm to 200 μm, the log differential intrusion increased as the

desert sand substitution ratio increased. Namely, high substitution ratios, such as 50 % and 100 %, of desert sand for the artificial aggregate slightly increased the concrete porosity. This finding was verified by Figure 5, the cumulative intrusion curves of the AS, DAS*, and DS concrete.

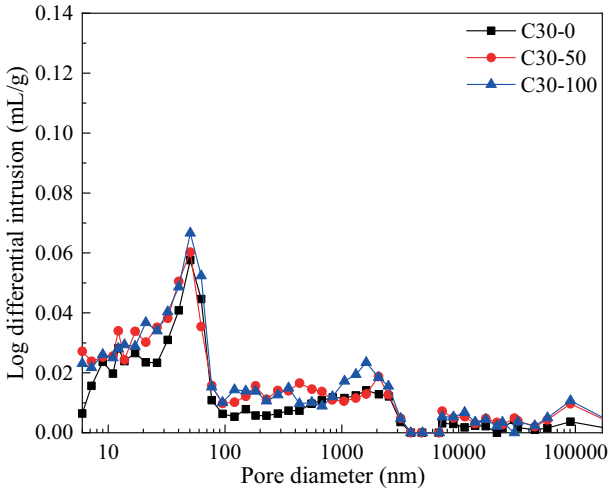

a) C30

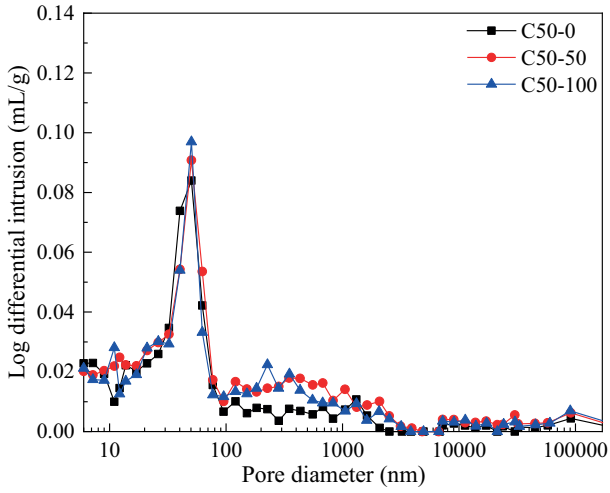

b) C50

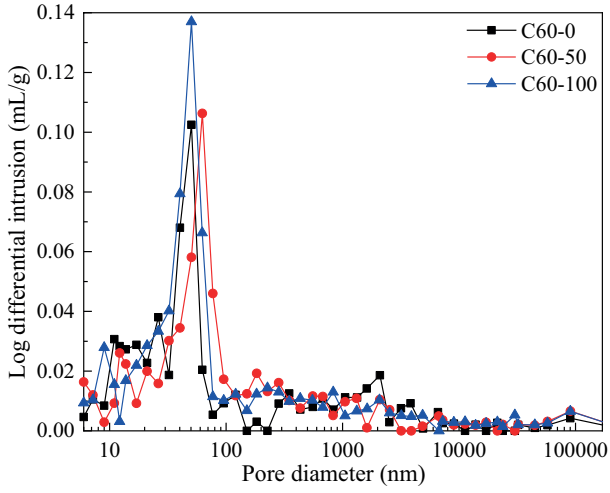

c) C60

Figure 4. Log differential intrusion of the AS, DAS and DS concrete.

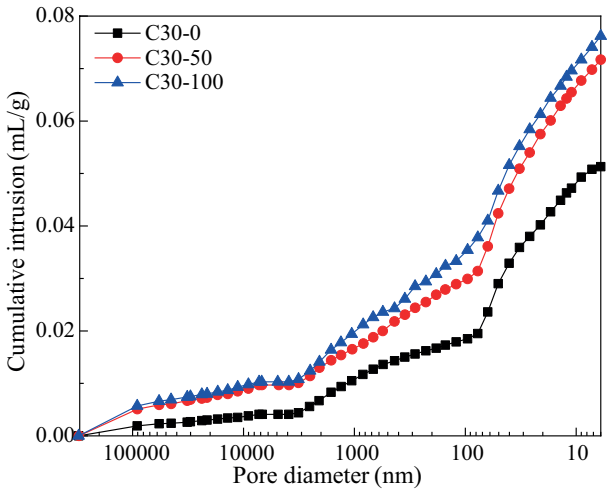

a) C30

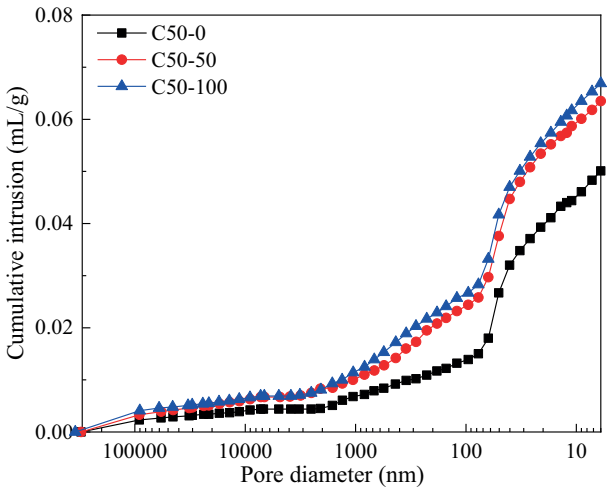

b) C50

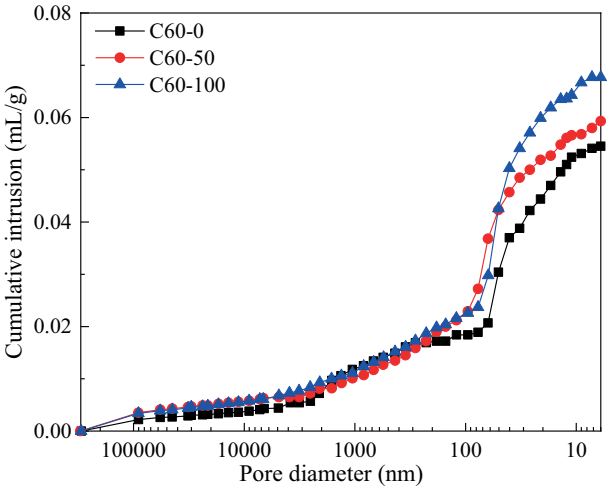

c) C60

Figure 5. Cumulative intrusion of the AS, DAS and DS concrete.

Figure 5 also shows that concrete with the desert sand had more pores with diameters less than 100 nm. It might be mistakenly considered as the higher hydration level of cement paste. Actually, it should be due to the reduction in the sand ratio with the desert sand substitution ratio increase (see Figure 3b). As the sand ratio decreased, the mortar specimens had more hardened cement paste and less sand, thus the porosity increased.

ITZ microhardness of DS concrete

The ITZ microhardness of the AS and DS concrete at various strength grades is shown in Figure 6. The ITZ widths are presented in Table 3.

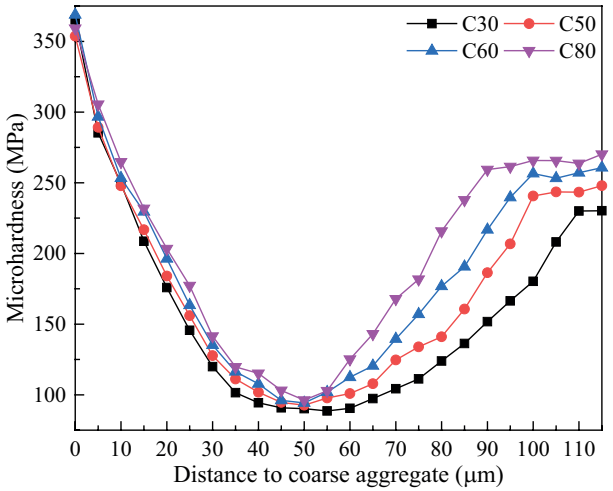

a) AS concrete

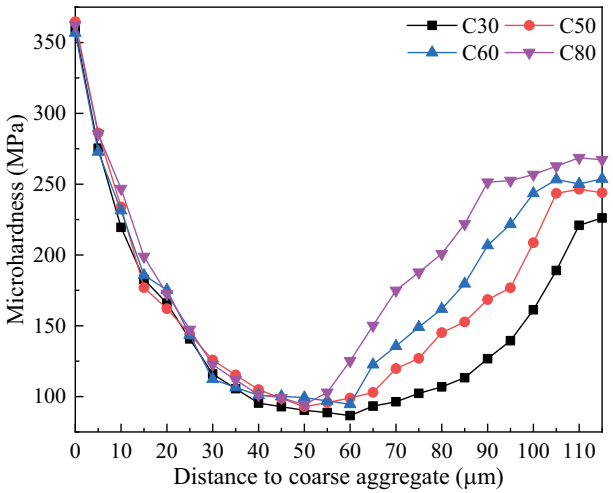

b) DS concrete

Figure 6. ITZ microhardness of the AS and DS concrete.

Table 3. ITZ widths of the AS and DS concrete (μm).

Concrete	C30	C50	C60	C80
RAS concrete	110	100	95	80
DS concrete	110	105	100	90

Obviously, the ITZ width decreased as the strength grade increased. Moreover, the microhardness of the cement paste matrix increased as the strength grade increased. Compared with the ITZ widths of the concrete with the artificial sand (Figure 6a) or natural river sand given in the published literature [22], the ITZ widths of the concrete using the desert sand in this study were larger [22]. It could be due to the soft and smooth surface (Figure 1) of the desert sand, which adversely affected the ITZ properties [9, 23].

Compressive strength of the DAS concrete

The compressive strength of the DAS concrete is shown in Figure 7. Figure 7a shows that desert sand substitution rarely affected the compressive strength of the C30 concrete. Each data point in the figure is the average of six data points, which came from three specimens, respectively.

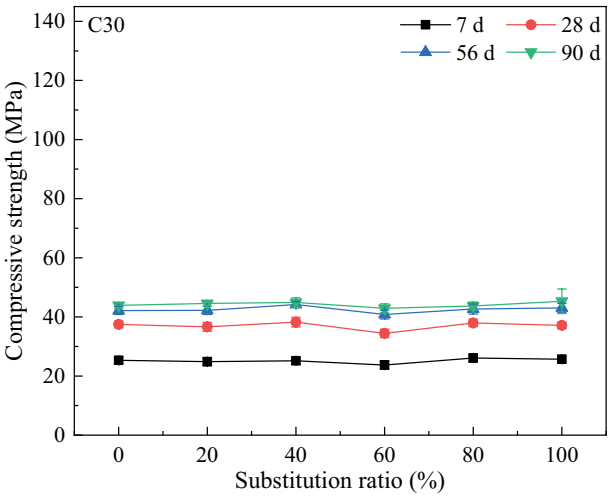

a) C30

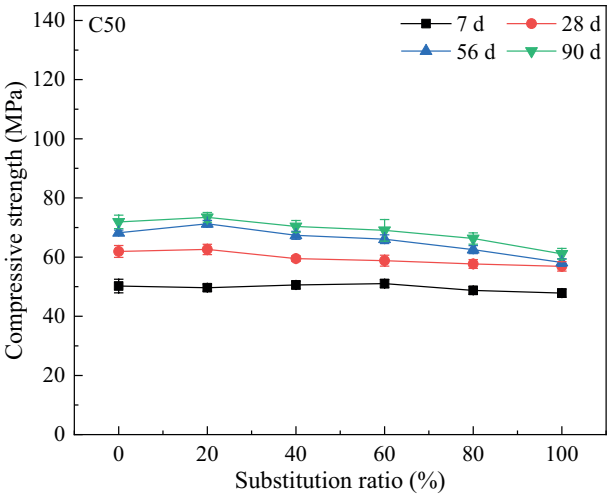

b) C50

Figure 7. Compressive strength of the DAS concrete. *(Continue on next page)*

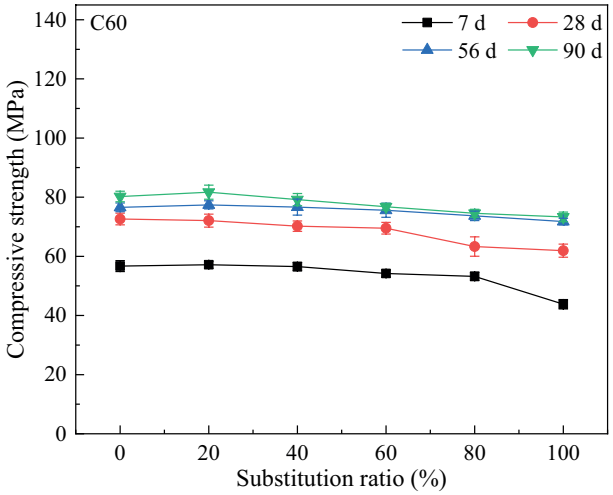

c) C60

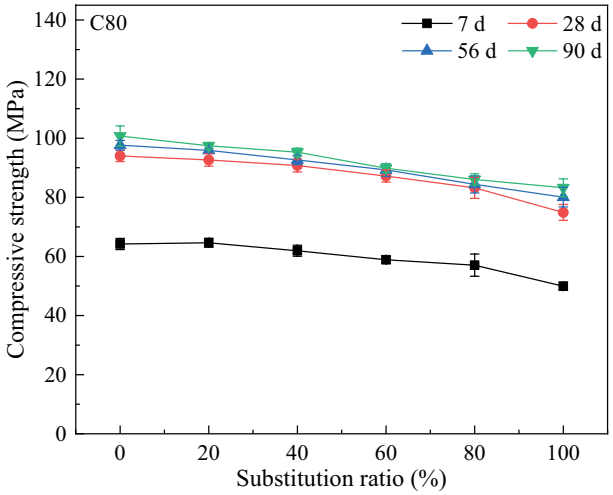

d) C80

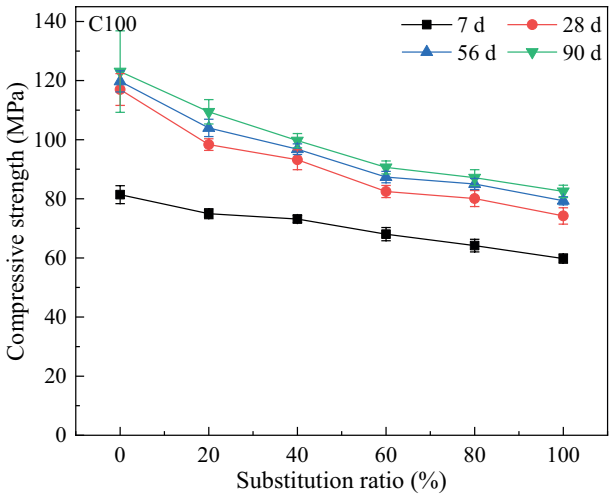

e) C100

Figure 7. Compressive strength of the DAS concrete.

As the concrete strength grade increased, the effect of the desert sand substitution was seen and gradually became more obvious. In general, the compressive strength decreased as the desert sand substitution ratio increased, however, for the C50 and C60 strength grades, the concrete with 20 % desert sand had a slightly higher strength compared with those without the desert sand substitution. Compared with the concrete with the 100 % desert sand and the concrete without the desert sand, the reduction ratios of the C50 and C60 concrete were 15.0 % and 8.6 % at the age of 90 days, respectively, while the reduction ratios of the C80 and C100 concrete were 17.4 % and 32.9 %, respectively. Figure 7d and e indicate that the desert sand should be cautiously used in the C80 and C100 concrete because the concrete strength might drop below the expected grades when the substitution ratios are high.

Generally, the desert sand substitution was not good for the concrete strength. However, it did present a slightly positive effect for the C60 or lower strength grade concrete if the substitution ratio was 20 %, as used in this study. For the consideration of the workability and economy, the concrete with the lower strength grade had a higher sand ratio (see Figure 2b). Namely, the artificial sand occupied a larger space in the concrete. As it is known, the particle-size distribution of artificial sand is always defective, mainly reflected by the lack of fine particles [24-26]. In this case, the application of desert sand doped artificial sand as the fine aggregate could bring a positive effect on the concrete strength as it improved the compactness of the concrete aggregate and delivered a denser structure. However, if the substitution ratio was too high or all the artificial sand was replaced by desert sand, the strength decreased due to the desert sand being too fine to form a reasonable aggregate gradation with the coarse aggregate [27].

Durability of the DAS concrete

Cl^- penetration resistance of the DAS concrete

The Cl^- penetrability of the DAS concrete was assessed by electric flux. The electric fluxes of the DAS concrete are shown in Figure 8. Each data point in the figure is an average of three data points, which were acquired from three specimens, respectively.

Figure 8 clearly shows that there was a negative correlation between the electric flux and the concrete strength grade. As the curing time increased, the electric fluxes of the DAS concrete decreased further. The electric fluxes of the high strength concrete (> C60) after 56 days of curing were less than 700 C, which indicated good impenetrability. For the C30 DAS concrete, electric fluxes of the concrete with various desert sand substitution ratios fluctuated and no clear tendency was delivered. The DAS concrete with 20 % desert sand showed less electric flux than the concrete without the desert sand, however, as the desert sand substitution ratio increased, the electric flux increased with the fluctuations except for the C30 concrete. The effect of the desert sand substitution ratio on the concrete impenetrability was found to be similar to the concrete compressive strength.

The reasons behind these effects should be the change in the compactness.

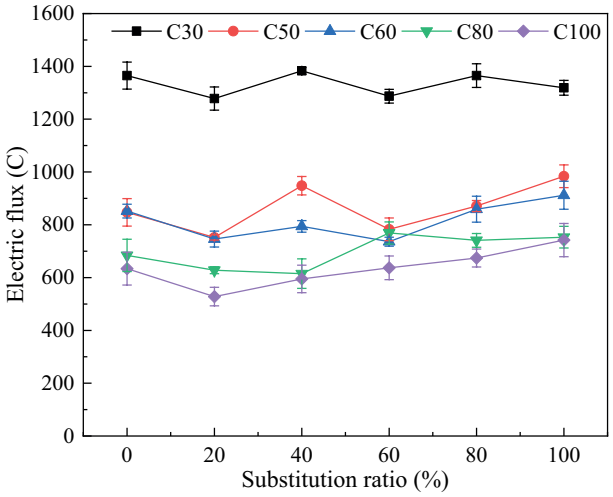

a) 28 d

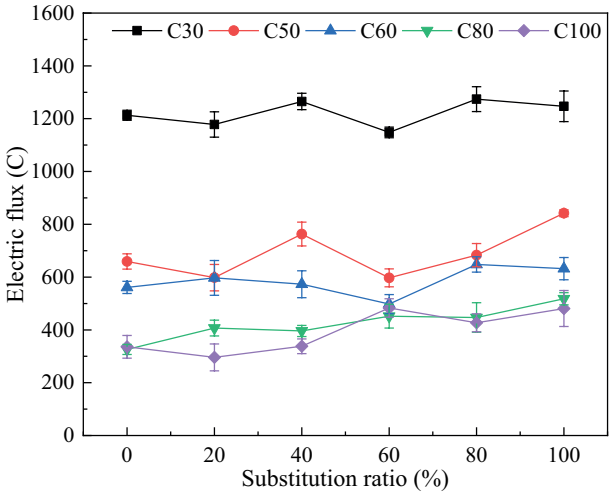

b) 56 d

Figure 8. Electric flux of the DAS concrete.

Frost resistance of the DAS concrete

The mass loss variations of the DAS concrete experienced by the freeze-thaw cycles are shown in Figure 9, while the simultaneous relative dynamic moduli variations are shown in Figure 10. Each data point in the figure is an average of three data points, which were obtained from three specimens, respectively.

In Figure 9, the mass loss increased as the freeze-thaw cycles increased. Also, the increased rate of mass loss was negatively correlated to the concrete strength grade. Except for the C30 DAS concrete, the mass losses of the DAS concrete in the other strength grades were less than 5 % after 475 freeze-dry cycles, indicating that they were still serviceable. The substitution of desert sand adversely affected the frost resistance of the concrete. Basically, as the desert sand substitution ratio increased, the frost resistance of the concrete became

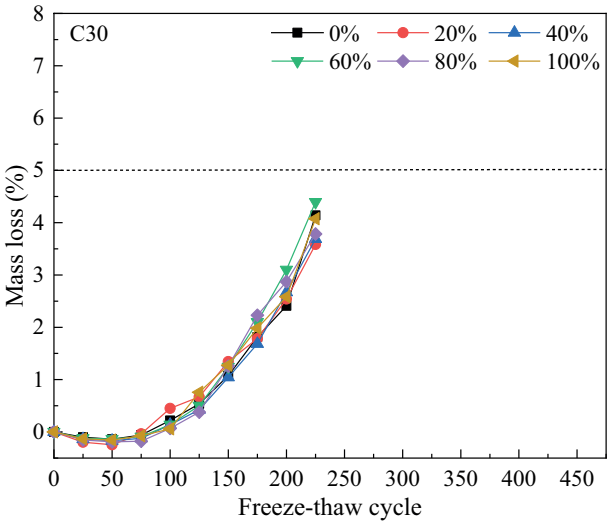

a) C30

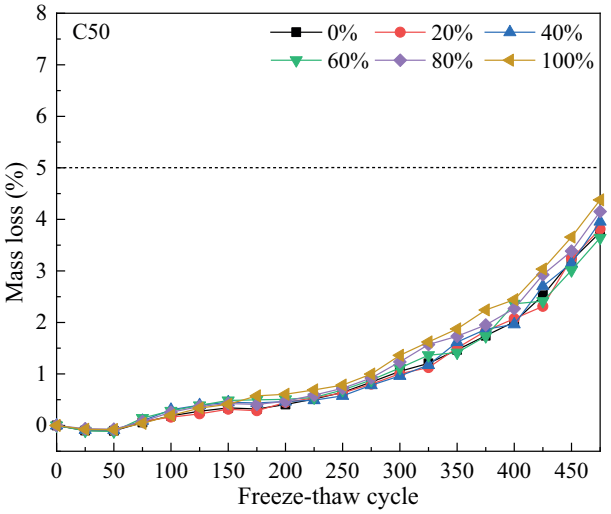

b) C50

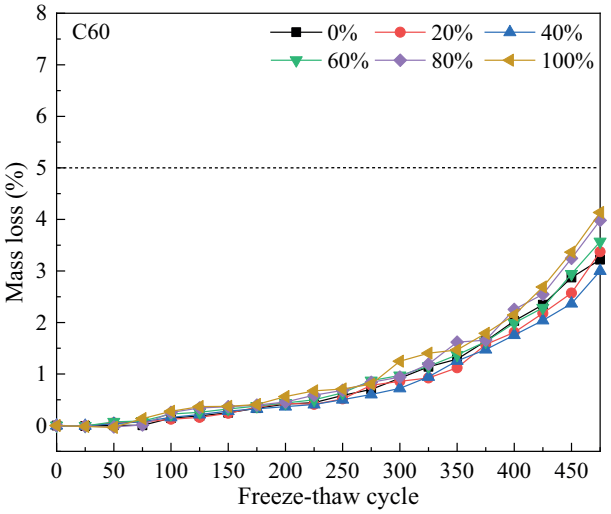

c) C60

Figure 9. Mass loss of the DAS concrete during the freeze-thaw cycling. *(Continue on next page)*

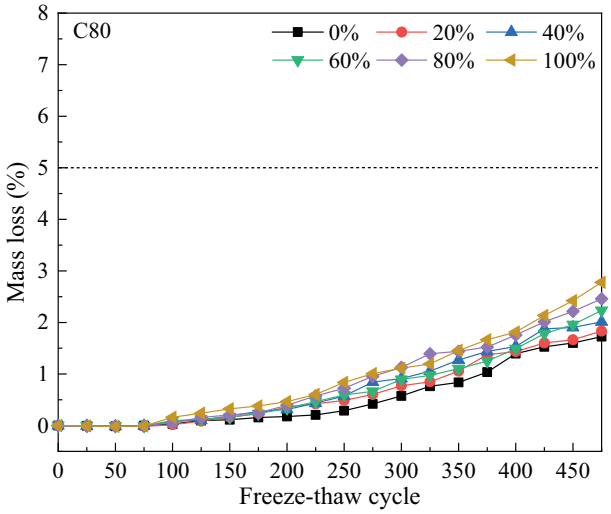

d) C80

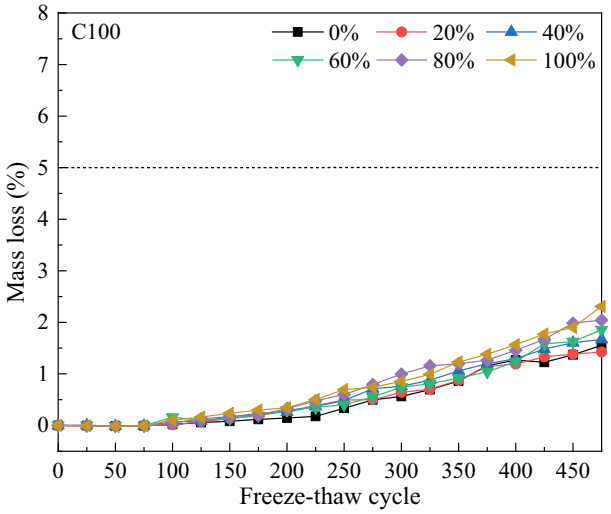

e) C100

Figure 9. Mass loss of the DAS concrete during the freeze-thaw cycling.

slightly worse. It should be noted that the substitution ratio of the desert sand increased the air content of the concrete, see Figure 3b, which generally indicated the superior frost resistance [28]. Therefore, the frost resistance improvement theory based on air entrainment was not suitable for the DAS concrete.

In Figure 10, the relative dynamic elastic decreased as the freeze-thaw cycles increased with fluctuations. Also, the rate of the decrease of the relative dynamic elastic modulus was negatively correlated to the concrete strength grade. The relative dynamic elastic moduli of the C30 DAS concrete were below 60 % after 200 freeze-thaw cycles, although the mass losses did not exceed 5 % at that time (Figure 9a). Except for the C30 DAS concrete, the DAS concrete in the other strength grades were still serviceable after 475 freeze-thaw cycles as their relative dynamic elastic moduli were still more than 60 %. In general, similar to the mass losses,

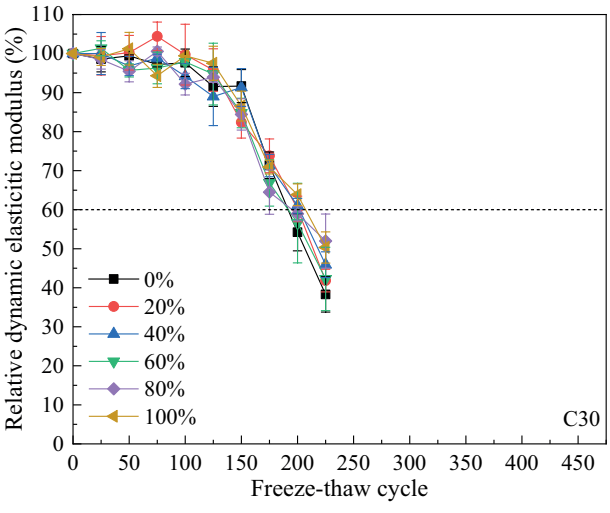

a) C30

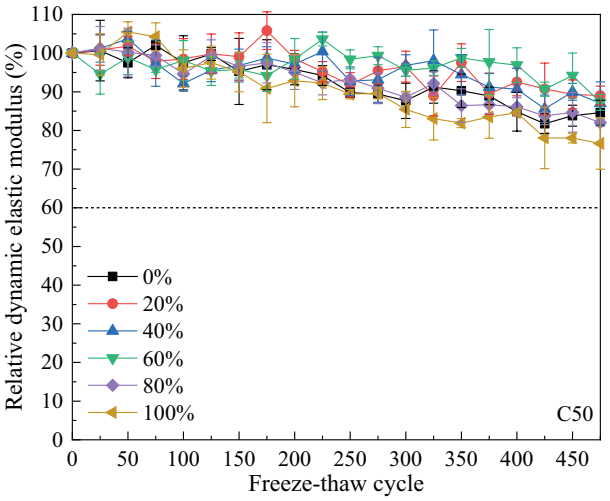

b) C50

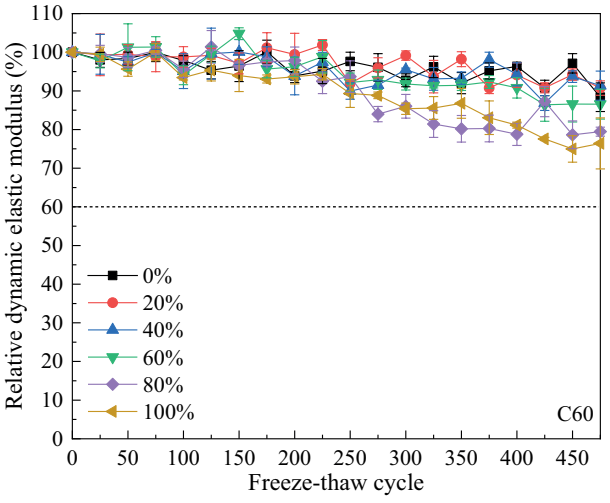

c) C60

Figure 10. Relative dynamic elastic modulus loss of the DAS concrete during the freeze-thaw cycling. *(Continue on next page)*

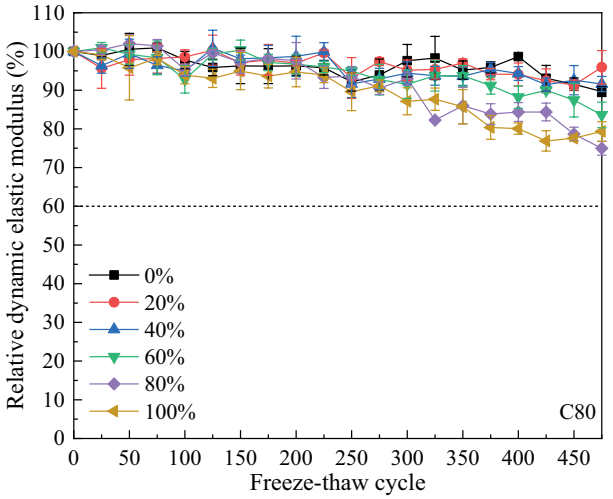

d) C80

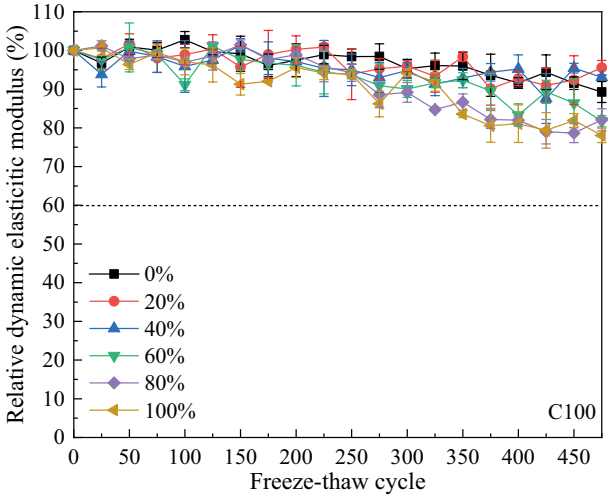

e) C100

Figure 10. Relative dynamic elastic modulus loss of the DAS concrete during the freeze-thaw cycling.

the relative dynamic elastic moduli reduced faster with the increase in the desert sand substitution ratio, also indicating that the desert sand substitution was not good for the frost resistance of the concrete. However, the concrete without the desert sand and the DAS concrete with the 20 % desert sand resembled each other in both the mass losses and the relative dynamic elastic modulus reductions. Hence, a low substitution ratio of desert sand to artificial sand would not significantly affect the frost resistance of the concrete.

Sulfate resistance of the DAS concrete

The strength variations of the DAS concrete experiencing a sulfate attack coupled with the wet-dry cycles are shown in Figure 11. Each data point in the figure is an average of three data points, which were obtained from three specimens, respectively. After 150 cycles, the residual strength ratios ranged from 82 % to 94 %. As the concrete strength grade increased, the resistance to the sulfate attack improved, although the error bars in the figure show that the errors of the residual strength ratios are very large.

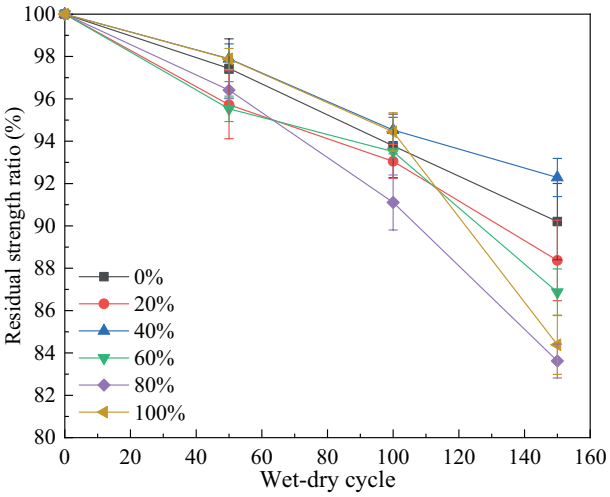

a) C30

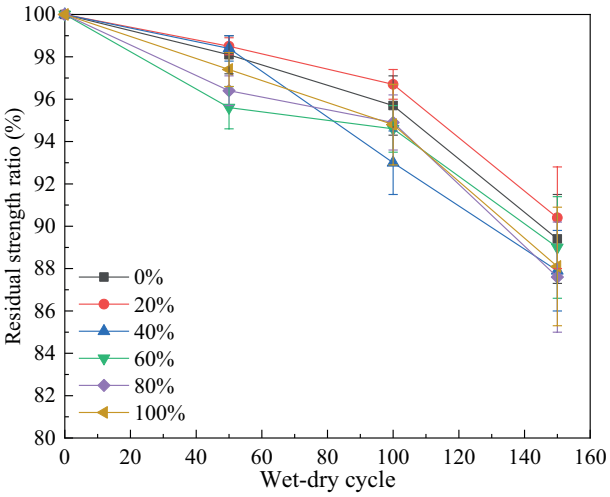

b) C50

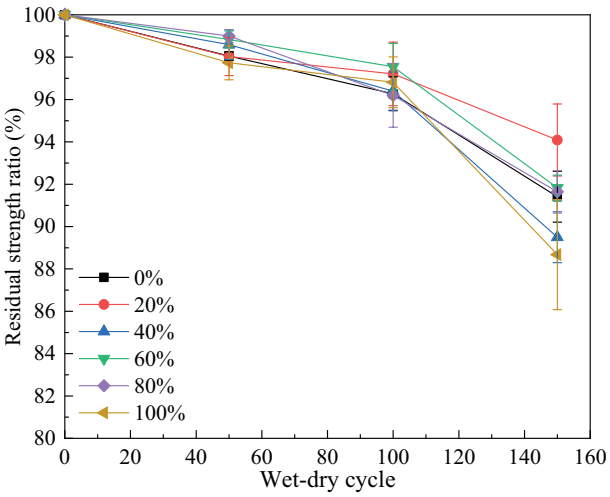

c) C60

Figure 11. Residual strength of the DAS concrete experiencing a sulfate attack. *(Continue on next page)*

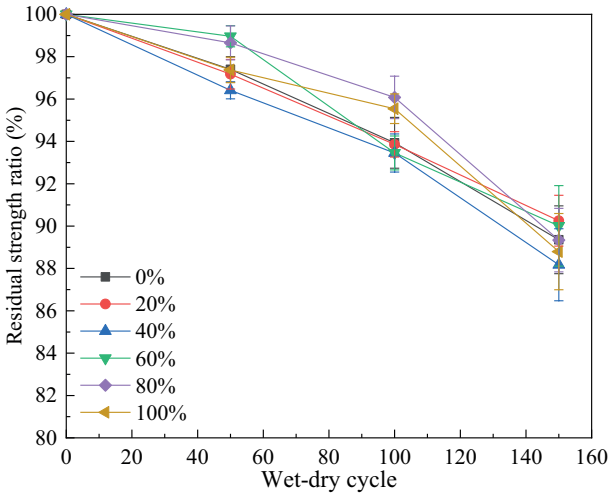

d) C80

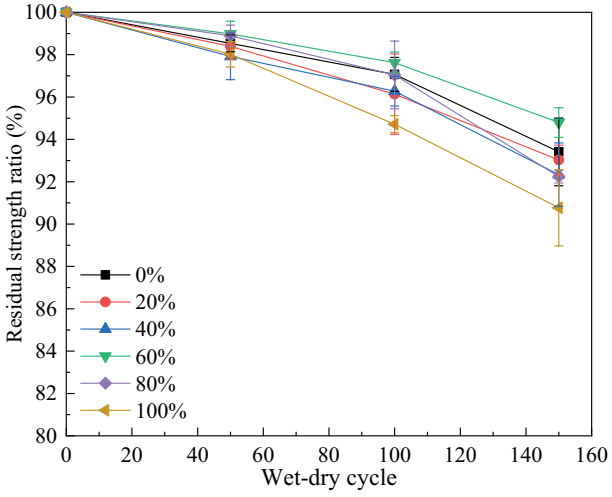

e) C100

Figure 11. Residual strength of the DAS concrete experiencing a sulfate attack.

In Figure 11, it can be found that the 100 % substitution of desert sand for the fine aggregate led to the weaker resistance to a sulfate attack in most cases. However, beyond that, there was no obvious regularity of the effect of the desert sand substitution ratio on the residual strength ratio of the concrete experiencing a sulfate attack. Errors in the investigation of the resistance to a sulfate attack might be due to the inharmonious deformation of the interface between the mortar and the coarse aggregate during the temperature cycles, which was coupled with the wet-dry cycles [29]. However, the effects of the desert sand on thermo-physical properties of the concrete were not covered in this study.

Drying shrinkage of the DAS concrete

The drying shrinkages of the DAS concrete are shown in Figure 12. Each data point in the figure is an average of three data points, which were obtained from three specimens, respectively. The mechanism of the drying shrinkage of the concrete is the capillary force of the pore system, thus, the factors affecting the concrete pore structure also affect the drying shrinkage of the concrete. For example, the drying shrinkage is

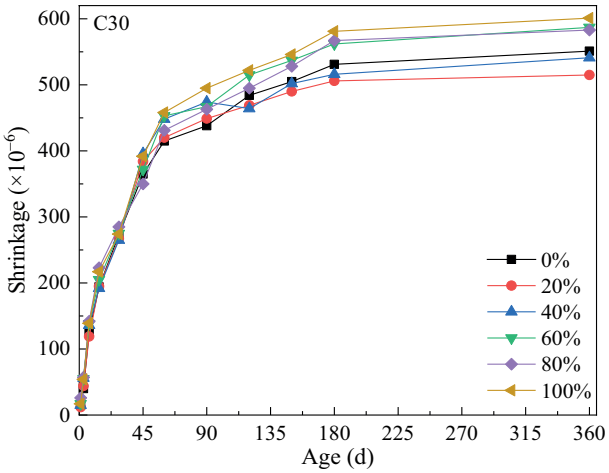

a) C30

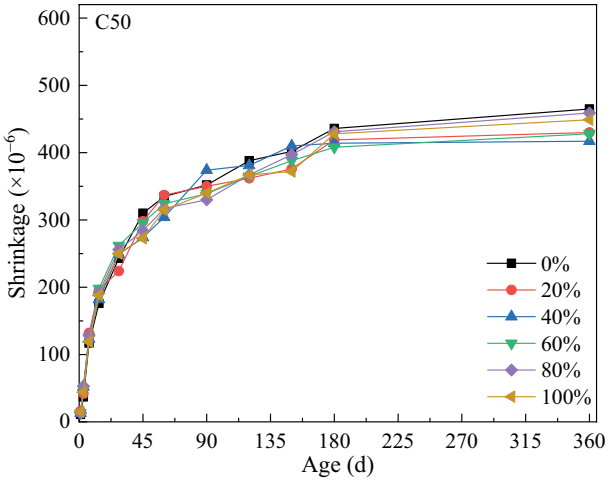

b) C50

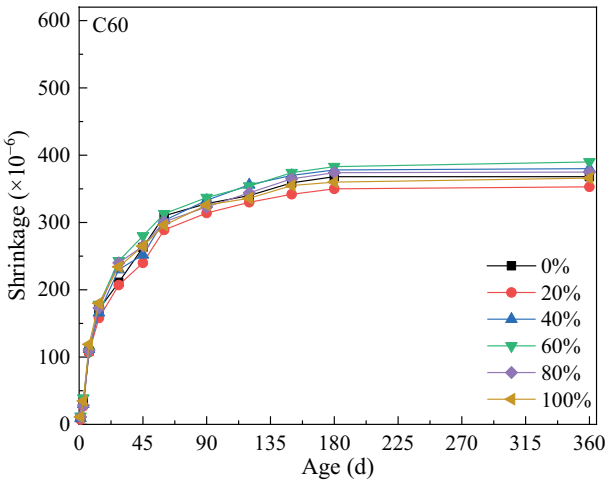

c) C60

Figure 12. Drying shrinkage of the DAS concrete. *(Continue on next page)*

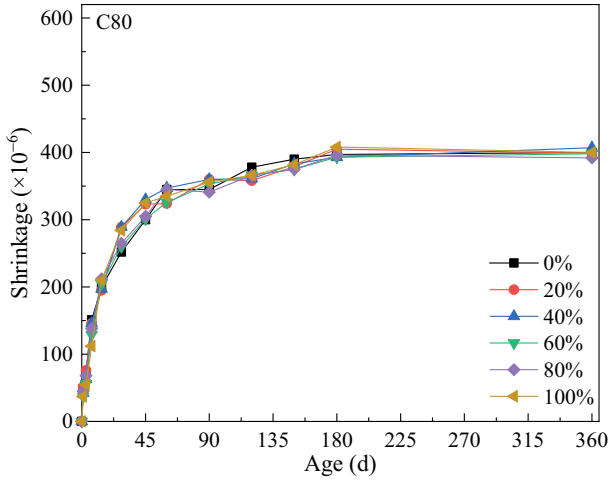

d) C80

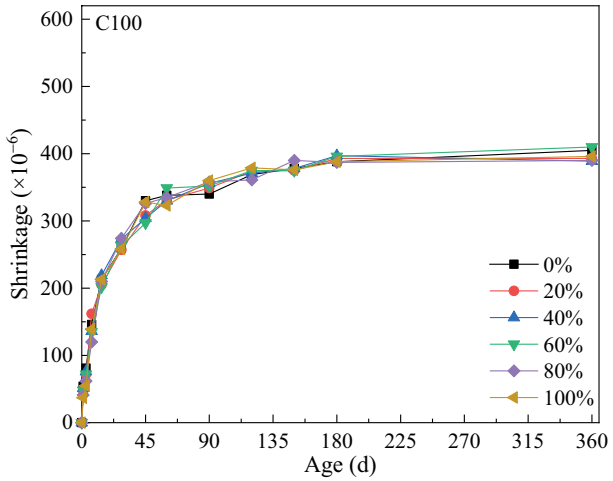

e) C100

Figure 12. Drying shrinkage of the DAS concrete.

positively correlated to the water/binder ratio [30], sand ratio [31], and the aggregate porosity [32, 33]. As the water absorption rate by the saturated surface dry state of the desert sand was obviously lower than that of artificial sand in this study (Table 1), the substitution of desert sand would not increase the total porosity of the aggregate. Some mineral additions, such as silica fume, would also accelerate the concrete shrinkage [34, 35]. In Figure 12a, b, c, the drying shrinkage of the concrete decreased as the concrete strength grade increased. It was due to reductions in the water/binder ratio and sand ratio, even though the binder mass also increased. However, in Figure 12c, d, e, the drying shrinkage of the concrete increased as the concrete strength grade increased slightly, which might be due to the addition of the silica fume.

Since the number of fine particles in the artificial sand was never enough, the substitution of fine desert sand might optimise the particle size distribution of the fine aggregate [9]. For the concrete having strength grades below C60, the appropriate substitution ratios of desert sand in the fine aggregate were good for the volume stability of the concrete. Generally, the DAS concrete with 20 % desert sand shrank more slowly than the concrete without the desert sand, although it was hard to determine that 20 % was the optimal substitution ratio. For the C30, C50, and C60 concrete with 20 % desert sand, the drying shrinkages at the age of 360 days were, respectively, reduced by 6.5 %, 7.5 %, and 4.1 %. The reduction effect of the 20 % desert sand on the drying shrinkage could be due to the denser structure, which corresponded to the improvement effect of the 20 % desert sand on the compressive strength of the C30, C50, and C60 concrete. The drying shrinkages of the C80 and C100 concrete at the age of 360 days were approximately 400 × 10^{-6}. There were neither obvious positive nor negative effects of the desert sand on drying shrinkage in the C80 and C100 concrete. Therefore, it could be concluded that the drying shrinkage of the common strength concrete (< C60) was more sensitive to the desert sand substitution than the high strength concrete (> C60).

CONCLUSIONS

The study conducted experiments on concrete using desert sand-doped artificial sand as the fine aggregate. The concrete strength grades included C30, C50, C60, C80, and C100, while the desert sand substitution ratios included 0 %, 20 %, 40 %, 60 %, 80 %, and 100 %. The slump values of all the investigated concrete were between 190 mm and 210 mm. The conclusions drawn from the study include the following:

- The high substitution ratios of desert sand, such as 50 % and 100 %, slightly increased the capillary porosity of the concrete and extended the ITZ width between the coarse aggregate and the cement mortar matrix.
- In general, the compressive strength decreased as the desert sand substitution ratio increased, however, for the C50 and C60 strength grades, the concrete with 20 % desert sand had slightly higher strength compared with those without the desert sand substitution.
- The concrete with the 20 % desert sand showed less electric flux than the concrete without the desert sand, however, as the desert sand substitution ratio increased, the electric flux increased with the fluctuations except for the C30 concrete. The substitution of desert sand adversely affected the frost resistance of the concrete, but the effect of the low substitution ratio of the desert sand was negligible. A 100 % substitution of the desert sand for the fine aggregate led to the weaker resistance to sulfate attacks in most cases.
- Generally, concrete with 20 % desert sand shrank more slowly than the concrete without the desert sand, although it was hard to determine that 20 % was the optimal substitution ratio. The drying shrinkage of the

common strength concrete (< C60) was more sensitive to the desert sand substitution than the high strength concrete (> C60).

- For the DAS concrete with strength grades from C30 to C60, the 20 % substitution ratio of desert sand brought slightly positive effects, while higher substitution ratios up to 60 % could still be acceptable. When further increasing the substitution ratio, the concrete properties might be negatively affected. In the case of the C80 DAS concrete, the substitution of desert sand generally brought negative effects and it was also suggested not to exceed the substitution ratio 60 %. Lastly, desert sand is not recommended in the C100 concrete.

Appendix A

Risk assessment of an alkali-silica reaction

As desert sand might contain active SiO_2, the risk assessment of an alkali-silica reaction is very important. The test was conducted in accordance with section 7.16.2 (rapid alkali-silica reaction) of GB/T 14684-2011: Sand for construction. However, the particle-size distribution of the desert sand was non-standard because the percentage of particles with a diameter larger than 600 nm in the studied desert sand was less than 1 %. There were four kinds of particle-size distributions in the assessment, see Table A1. The risk assessment of the alkali-silica reaction was delivered based on the 14 d expansivity of mortar prisms with different categories of sand and different particle-size distributions, see Table A2.

Additionally, many literature sources have pointed out that a certain pessimum exists for which the pressure or expansivity of a mortar with an alkali-silica reaction is the maximum [36,37]. If the majority of the desert sand particles is smaller than the pessimum, the harmful effect of an alkali-silica reaction on the concrete durability would be less significant, even if there are some active SiO_2.

Acknowledgements

The authors appreciate the financial support from China Railway 20th Bureau Group Corporation Limited.

REFERENCES

1. Bendixen M., Best J., Hackney C., Iversen L. L. (2019): Time is running out for sand. *Nature, 571*, 29-31. doi: 10.1038/d41586-019-02042-4.
2. Torres A., Brandt J., Lear K., Liu J. G. (2017): A looming

Table A1. Mix proportion of the cement paste for the DAS concrete.

Distribution No.	75~150 (μm)	150~200 (μm)	200~300 (μm)	300~600 (μm)	0.6~1.18 (mm)	0.6~2.36 (mm)	2.36~4.75 (mm)	Total (μm)
D1	198.0	495.0	297.0					
D2	198.0	297.0	297.0	198.0				990.0
D3		148.5	148.5	247.5	247.5	247.5	99.0	
D4	Natural particle-size distribution							

Note: D3 is the standard distribution specified by GB/T 14684-2011.

Table A2. Risk assessment of the alkali-silica reaction.

Category	Particle-size distribution	14 d expansivity of mortar prism (%)	Risk assessment of the alkali-silica reaction
River sand	D1	0.01661	14 d expansivity<0.10%, assessed as safe according to GB/T 14684-2011
	D2	0.02804	
	D3	0.03420	
Artificial sand	D1	0.03759	
	D2	0.04355	
	D3	0.07682	
Desert sand	D1	0.01961	
	D2	0.02691	
	D4	0.02477	

Note: 1. The river sand here was from the Wei River.
2. The mortar prism was 25 mm × 25 mm × 280 mm in size.
3. The mass ratio of the cement: water: sand was 1: 0.47: 2.25. For a group of three mortar prisms, the masses of the cement and mortar were, respectively, 440 g and 990 g.
4. In the curing stage, the mortar prisms were immersed in a 1 mol/L NaOH solution, which was kept at 80 ℃.

tragedy of the sand commons. *Science, 357*, 970-971. doi: 10.1126/science.aao0503.
3. Santhosh K. G., Subhani S. M., Bahurudeen A. (2021): Cleaner production of concrete by using industrial by-products as fine aggregate: A sustainable solution to excessive river sand mining. *Journal of Building Engineering, 42*, 102415. doi: 10.1016/j.jobe.2021.102415.
4. Dhondy T., Remennikov A., Sheikh M. N. (2020): Properties and Application of Sea Sand in Sea Sand-Seawater Concrete. *Journal of Materials in Civil Engineering, 32*, 04020392. doi: 10.1061/(Asce)Mt.1943-5533.0003475.
5. Wang X. M., Chen F., Hasi E., Li J. C. (2008): Desertification in China: An assessment. *Earth-Science Reviews, 88*, 188-206. doi:10.1016/j.earscirev.2008.02.001.
6. Zhang M. H., Zhu X. Z., Shi J. Y., Liu B. J., He Z. H., Liang C. F. (2022): Utilization of desert sand in the production of sustainable cement-based materials: A critical review. *Construction and Building Materials, 327*, 127014. doi: 10.1016/j.conbuildmat.2022.127014.
7. Zhang G. X., Song J. X., Yang J. S., Liu X. Y. (2006): Performance of mortar and concrete made with a fine aggregate of desert sand. *Building and Environment, 41*, 1478-1481. doi: 10.1016/j.buildenv.2005.05.033.
8. Wang, J.R., Ou, Z.W., Liu, J.M., Xiong, Z.Q., Wang, J.W., Wang, Y.Y., Luo, W., Liu, Y. (2019): Study on durability of ultra high performances concrete with aeolian sand. *IOP Conference Series: Earth and Environmental Science, 300*, 22017. doi:10.1088/1755-1315/300/2/022017.
9. Jiang J. Y., Feng T. T., Chu H. Y., Wu Y. R., Wang F. J., Zhou W. J., Wang Z. F. (2019): Quasi-static and dynamic mechanical properties of eco-friendly ultra-high-performance concrete containing aeolian sand. *Cement & Concrete Composites, 97*, 369-378. doi: 10.1016/j.cemconcomp.2019.01.011.
10. Nécira, B.,Guettala, A., Guettala, S. (2017): Study of the combined effect of different types of sand on the characteristics of high performance self-compacting concrete. *Journal of adhesion science and Technology, 31*, 1912-1928. doi: 10.1080/01694243.2017.1289829.
11. Benabed B., Kadri E. H., Azzouz L., Kenai S. (2012): Properties of self-compacting mortar made with various types of sand. *Cement & Concrete Composites, 34*, 1167-1173. doi: 10.1016/j.cemconcomp.2012.07.007.
12. Li Y. G., Zhang H. M., Liu X. Y., Liu G. X., Hu D. W., Meng X. Z. (2019): Time-Varying Compressive Strength Model of Aeolian Sand Concrete considering the Harmful Pore Ratio Variation and Heterogeneous Nucleation Effect. *Advances in Civil Engineering, 2019*, 5485630. doi: 10.1155/2019/5485630.
13. Li Y. G., Zhang H. M., Liu G. X., Hu D. W., Ma X. R. (2020): Multi-scale study on mechanical property and strength prediction of aeolian sand concrete. *Construction and Building Materials, 247*, 118538. doi: 10.1016/j.conbuild-mat.2020.118538.
14]Wang, X.Y., Liu, M.H., Liu, X., Jia,S.Y., Xu,Z. (2022): Study on mechanical properties and carbon emissions of desert sand and machine – made sand concrete. *China Civil Engineering Journal, 55*, 23-30. doi: 10.15951/j.tmgcxb.2022.02.010.
15. Che J. L., Wang D., Liu H. F., Zhang Y. X. (2019): Mechanical Properties of Desert Sand-Based Fiber Reinforced Concrete (DS-FRC). *Applied Sciences-Basel, 9*, 1857. doi: 10.3390/app9091857.
16. Amel C. L., Kadri E. H., Sebaibi Y., Soualhi H. (2017): Dune sand and pumice impact on mechanical and thermal lightweight concrete properties. *Construction and Building Materials, 133*, 209-218. doi: 10.1016/j.conbuildmat.2016.12.043.
17. Luo F. J., He L., Pan Z., Duan W. H., Zhao X. L., Collins F. (2013): Effect of very fine particles on workability and strength of concrete made with dune sand. *Construction and Building Materials, 47*, 131-137. doi: 10.1016/j.conbuildmat.2013.05.005.
18. Liu H. F., Ma Y. C., Ma J. R., Yang W. W., Che J. L. (2021): Frost Resistance of Desert Sand Concrete. *Advances in Civil Engineering, 2021*, 1-17. doi: 10.1155/2021/6620058.
19. Zhang M. H., Liu H. F., Sun S., Chen X. L., Doh S. I. (2019): Dynamic Mechanical Behaviors of Desert Sand Concrete (DSC) after Different Temperatures. *Applied Sciences-Basel, 9*, 4151. doi: 10.3390/app9194151.
20. Al-Harthy A. S., Halim M. A., Taha R., Al-Jabri K. S. (2007): The properties of concrete made with fine dune sand. *Construction and Building Materials, 21*, 1803-1808. doi: 10.1016/j.conbuildmat.2006.05.053.
21. Benabed B., Azzouz L., Kadri E., Kenai S., Belaidi A. S. E. (2014): Effect of fine aggregate replacement with desert dune sand on fresh properties and strength of self-compacting mortars. *Journal of Adhesion Science and Technology, 28*, 2182-2195. doi: 10.1080/01694243.2014.950625.
22. Li Y. G., Zhang H. M., Chen S. J., Wang H. R., Liu G. X. (2022): Multi-scale study on the durability degradation mechanism of aeolian sand concrete under freeze-thaw conditions. *Construction and Building Materials, 340*, 127433. doi: 10.1016/j.conbuildmat.2022.127433.
23. Liu X. Y., Liu R. D., Lyu K., Gu Y. (2022): A Quantitative Evaluation of Size and Shape Characteristics for Desert Sand Particles. *Minerals, 12*,581. doi: 10.3390/min12050581.
24. Gnanasaravanan S., Rajkumar P. (2013): Characterization of minerals in natural and manufactured sand in Cauvery River belt, Tamilnadu, India. *Infrared Physics & Technology, 58*, 21-31. doi: 10.1016/j.infrared.2012.12.042.
25. Goncalves J. P., Tavares L. M., Toledo R. D., Fairbain E. M. R., Cunha E. R. (2007): Comparison of natural and manufactured fine aggregates in cement mortars. *Cement and Concrete Research, 37*, 924-932. doi: 10.1016/j.cemconres.2007.03.009.
26. Celik T., Marar K. (1996): Effects of crushed stone dust on some properties of concrete. *Cement and Concrete Research, 26*, 1121-1130. doi: 10.1016/0008-8846(96)00078-6.
27. Liu H. F., Ma J. R., Wang Y. Y., Ning J. G. (2017): Influence of desert sand on the mechanical properties of concrete subjected to impact loading. *Acta Mechanica Solida Sinica, 30*, 583-595. doi: 10.1016/j.camss.2017.10.007.
28. Wang L., Guo F. X., Yang H. M., Wang Y., Tang S. W. (2021): Comparison of Fly Ash, Pva Fiber, Mgo and Shrinkage-Reducing Admixture on the Frost Resistance of Face Slab Concrete Via Pore Structural and Fractal Analysis. *Fractals-Complex Geometry Patterns and Scaling in Nature and Society, 29*, 21400028. doi: 10.1142/S0218348x21400028.
29. Standard for test methods of long-term performance and durability of ordinary concrete; GB 50082-2009; China Quality and Standards Publishing & Media Co., Ltd: Beijing, China, 2009.
30. Kioumarsi M., Azarhomayun F., Haji M., Shekarchi M. (2020): Effect of Shrinkage Reducing Admixture on Drying Shrinkage of Concrete with Different w/c Ratios. *Materials,*

13, 5721. doi: 10.3390/ma13245721.
31. Lee E., Park S., Kim Y. (2016): Drying shrinkage cracking of concrete using dune sand and crushed sand. *Construction and Building Materials, 126*, 517-526. doi: 10.1016/j.conbuildmat.2016.08.141.
32. Yukimasa GOTO., Tadashi FUJIWARA. (1976): Volumetric Change Of Aggregates By Absorption And Drying. *Proceedings of the Japan Society of Civil Engineers, 1976*, 97-108. doi: 10.2208/jscej1969.1976.247_97.
33. Zhang W. Y., Zakaria M., Hama Y. (2013): Influence of aggregate materials characteristics on the drying shrinkage properties of mortar and concrete. *Construction and Building Materials, 49,* 500-510. doi: 10.1016/j.conbuildmat.2013.08.069.
34. Mazloom M., Ramezanianpour A. A., Brooks J. J. (2004): Effect of silica fume on mechanical properties of high-strength concrete. *Cement & Concrete Composites, 26*, 347-357. doi: 10.1016/S0958-9465(03)00017-9.
35. Sadeghian G., Behfarnia K., Teymouri M. (2022): Drying shrinkage of one-part alkali-activated slag concrete. *Journal of Building Engineering, 51*, 104263. doi: 10.1016/j.jobe.2022.104263.
36. Binal A. (2015): The Pessimum Ratio and Aggregate Size Effects on Alkali Silica Reaction. *World Multidisciplinary Earth Sciences Symposium, Wmess 2015, 15,* 725-731. doi: 10.1016/j.proeps.2015.08.103.
37. Bazant Z. P., Steffens A. (2000): Mathematical model for kinetics of alkali-silica reaction in concrete. *Cement and Concrete Research, 30,* 419-428. doi: 10.1016/S0008-8846(99)00270-7.